

Mice lacking *Dfna5* show a diverging number of cochlear fourth row outer hair cells

Lut Van Laer,^a Markus Pfister,^b Sofie Thys,^a Karen Vrijens,^a Marcus Mueller,^b Lieve Umans,^c Lutgarde Serneels,^c Luc Van Nassauw,^d Frank Kooy,^a Richard J.H. Smith,^e Jean-Pierre Timmermans,^d Fred Van Leuven,^c and Guy Van Camp^{a,*}

^aDepartment of Medical Genetics, University of Antwerp, Campus Drie Eiken, Universiteitsplein 1, B-2610 Antwerp, Belgium

^bHals-Nasen-Ohrenklinik, Universität of Tübingen, Tübingen, Germany

^cExperimental Genetics Group, University of Leuven, Leuven, Belgium

^dLaboratory of Cell Biology and Histology, University of Antwerp, Campus Middelheim, Antwerp, Belgium

^eMolecular Otolaryngology Research Laboratories, University of Iowa, Iowa City, IA 52242-1182, USA

Received 9 November 2004; accepted 12 January 2005

Available online 2 March 2005

A complex mutation in *DFNA5*, resulting in exon 8 skipping, causes autosomal dominant hearing impairment, which starts in the high frequencies between 5 and 15 years of age and progressively affects all frequencies. To study its function in vivo, *Dfna5* knockout mice were generated through the deletion of exon 8, simultaneously mimicking the human mutation. To test the hearing impairment, frequency-specific Auditory Brainstem Response (ABR) measurements were performed at different ages in two genetic backgrounds (C57Bl/6J and CBA/Ca), but no differences between *Dfna5*^{-/-} and *Dfna5*^{+/+} mice could be demonstrated. Morphological studies demonstrated significant differences in the number of fourth row outer hair cells between *Dfna5*^{-/-} mice and their wild-type littermates. These results were obtained in both genetic backgrounds, albeit with opposite effects. In contrast to the results obtained in *Dfna5*^{-/-} zebrafish, we did not observe different UDP-glucose dehydrogenase and hyaluronic acid levels in *Dfna5*^{-/-} mice when compared to *Dfna5*^{+/+} mice.

© 2005 Elsevier Inc. All rights reserved.

Keywords: Hereditary hearing impairment; *DFNA5*; Knockout; Supernumerary hair cells

Introduction

Hearing loss is the most common sensory disability. Approximately 1 out of 500 newborns has congenital hearing loss (Mehl and Thomson, 1998, 2002). Another one in a thousand children will develop severe or profound hearing impairment before adulthood (Morton, 1991). In developed countries, more than half

of prelingual hearing loss are attributed to genetic factors (Marazita et al., 1993; Rehm, 2003). During the past decade, tremendous progress has been made in the field of human hereditary hearing loss. More than 100 loci have been mapped to the human genome and more than 40 responsible genes have been identified. An overview of all human hearing impairment loci and gene identifications can be found on the Hereditary Hearing Loss Homepage (Van Camp, G., Smith, R.J.H. Hereditary Hearing Loss Homepage. URL: <http://webhost.ua.ac.be/hhh/>).

The fifth autosomal dominant locus for hereditary hearing impairment, *DFNA5*, was mapped to chromosome 7p15 in an extended Dutch family in 1995 (Van Camp et al., 1995). The hearing loss that segregates in the family is progressive, non-syndromic, sensorineural and it starts in the high frequencies at an age of 5 to 15 years. Only at older ages do the lower frequencies become affected. In 1998, the gene responsible for this type of hearing impairment was identified (Van Laer et al., 1998). In a newly identified transcript that mapped to the *DFNA5* candidate region, a complex insertion/deletion mutation was detected in intron 7. At the mRNA level, this mutation causes skipping of exon 8, resulting in a frame shift and premature truncation of the protein. The gene was designated *DFNA5*, according to the corresponding locus, as no physiological function could be deduced despite extensive computational analysis (Van Laer et al., 1998). The gene was expressed in every tissue investigated so far, including the cochlea (Van Laer et al., 1998 and unpublished results).

The extended Dutch family in which *DFNA5* first was identified long remained the only *DFNA5* family. This has changed recently, with the description of a Chinese family (Yu et al., 2003) harboring a 3-nucleotide deletion in the polypyrimidine tract of intron 7 and a second Dutch family (Bischoff et al., 2004) with a nucleotide substitution in the splice-acceptor site of intron 7. In general, the hearing loss in the newly described families is very

* Corresponding author. Fax: +32 3 820 25 66.

E-mail address: Guy.VanCamp@ua.ac.be (G. Van Camp).

Available online on ScienceDirect (www.sciencedirect.com).

similar to that found in the original Dutch family. Only the reported age at onset differs slightly. It ranges from 0 to 40 years in the second Dutch family (Bischoff et al., 2004) and from 7 to 30 years in the Chinese family (Yu et al., 2003). Although at the genomic DNA level, the mutations in *DFNA5* leading to hearing loss are diverse, at the mRNA level, all these mutations lead to exon 8 skipping, indicating that only this particular event might cause hearing impairment. This fact, in combination with the fact that no other mutations in other parts of the gene have been described, led to the formulation of the hypothesis that *DFNA5*-associated hearing loss is caused by a gain-of-function mutation. The first lines of evidence supporting the hypothesis of a deleterious new function for mutant *DFNA5* have been gained very recently. It was demonstrated that human mutant *DFNA5* was toxic for yeast (Gregan et al., 2003) as well as for mammalian (Van Laer et al., 2004) cells.

Dfna5 function was investigated in zebrafish using morpholino antisense nucleotide technology (Busch-Nentwich et al., 2004). Zebrafish lacking *Dfna5* showed a disorganization of the developing semicircular canals and a reduction of the pharyngeal cartilage. A complete absence of UDP-glucose dehydrogenase (*Ugdh*) and a strong reduction in hyaluronic acid (HA) levels were demonstrated in the developing ear and pharyngeal arches of *Dfna5* knockout zebrafish. *Ugdh* is a key enzyme in the biosynthesis of glycosaminoglycans (and in particular of HA), the components of ground substance, which is the gel-like matrix that composes cartilage together with collagen and elastin fibers. The authors argue that *Dfna5* might regulate HA biosynthesis, which in turn might be essential for cartilage differentiation and correct outgrowth of the semicircular canals (Busch-Nentwich et al., 2004). As *DFNA5* is an orphan gene and until very recently nothing was known regarding its function (Van Laer et al., 1998), we decided to mimic the human mutation in the mouse through the deletion of exon 8 by targeted recombination in 129 ES cell lines. This mouse, which turned out to be a *Dfna5* knockout, was characterized audiologically and morphologically. The results obtained in *Dfna5* knockout zebrafish (Busch-Nentwich et al., 2004) could not be confirmed in *Dfna5* knockout mice.

Material and methods

Construction of a *Dfna5h* targeting vector

A 129SV mouse genomic λ FIXTM II library (Stratagene, La Jolla, CA) was screened with a 130 bp, exon 8-containing hybridization probe that was PCR-generated using exon8-F (5'-GACAGTCAGCAGCAGGACC-3') and exon8-R (5'-CGCTG-ACCAGGAAGTAGGC-3'), and the previously cloned mouse *Dfna5h* as template (Van Laer et al., 1998). Three positive clones were purified and the length of the inserts was determined by separating *NotI* restriction fragments with FIGE (FIGE-mapper, Bio-Rad, Hercules, CA). The longest insert (16 kb), containing exons 5 to 9 as determined by PCR using exon-derived primers (all exon primer sequences available on request), was chosen for further characterization and cloned into pBluescript plasmid (Stratagene, La Jolla, CA). A restriction map was obtained using a combination of sequencing with exon primers, long-range PCR (Advantage cDNA PCR kit; Clontech, BD Biosciences, Palo Alto, CA) with exon primers to determine the length of the introns and

finally Southern blotting using the different exons as hybridization probes. All sequencing reactions were performed using the Big-Dye Dye-Terminator Cycle Sequencing Kit (Applied Biosystems, Foster City, CA) and a 377 DNA sequencer (Applied Biosystems, Foster City, CA). A 6.5 kb *HindIII* fragment, containing exons 6 to 8, was chosen for further engineering and was subcloned into pBluescript. Long-range PCR with exon 6 or exon 8 and pBluescript primers was used to determine the length of the DNA stretches between the respective exons and the vector, after which the construction was initiated (Fig. 1A). A first *LoxP* site was inserted in an *SstI* site between exons 6 and 7. Subsequently, exon 8 was deleted by restriction digestion with 2 rare cutters (*MunI*, Roche, Basel, Switzerland and *Bsp119I*, Fermentas, Vilnius, Lithuania), for which the restriction sites are located in the neighborhood of the 5' and the 3' end of exon 8 respectively, and replaced with a cassette containing the hygromycin resistance gene under control of the phosphoglycerate kinase (PGK) promoter (te Riele et al., 1990), flanked by 2 *LoxP* sites. Finally, exons 6 and 7 were resequenced to exclude the occurrence of errors during the different construction steps. 1.8 and 0.7 kb were available for homologous recombination at the 5' and the 3' end of the 6.5 kb *HindIII* subclone, respectively.

Generation of the *Dfna5*^{-/+} and *Dfna5*^{-/-} mice

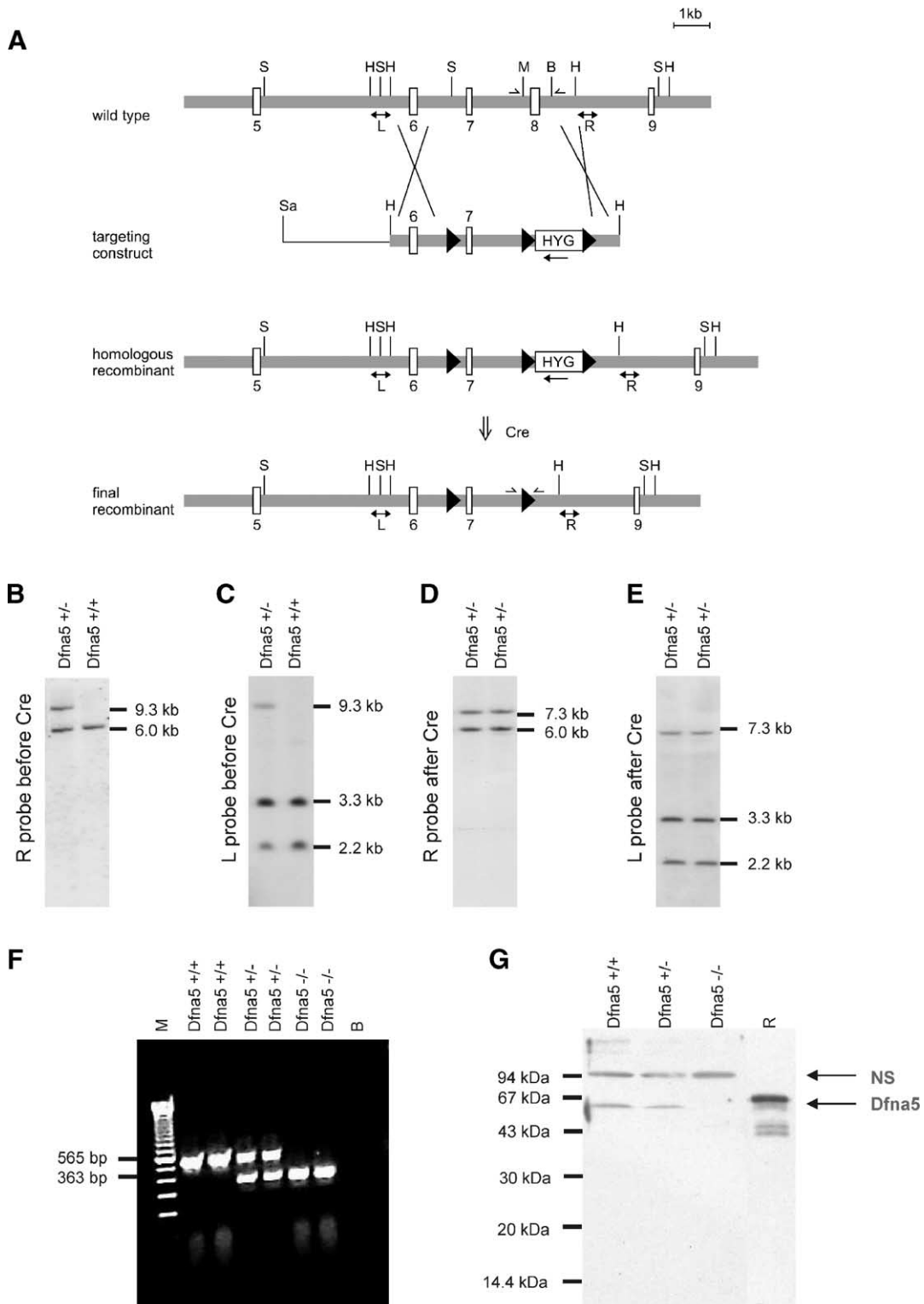
ES cell line E14 (Hooper et al., 1987) was cultured on mitomycin-treated STO fibroblast feeder layers as described before (Hooper et al., 1987; Umans et al., 1994). After linearization of the construct using the unique *SaI* site, 10 μ g was electroporated into 1.5×10^7 ES cells. Fourteen days after electroporation and selection in hygromycin B-containing (100 μ g/ml; Duchefa Biochemie, The Netherlands) medium, resistant clones were picked, expanded, frozen and analyzed for homologous recombination at the *Dfna5h* locus by Southern blotting. For this purpose, 15 μ g genomic DNA was digested with *SstI*, blotted and hybridized with probes located externally of either end of the targeting construct as indicated in Fig. 1A. The probe at the upstream 5'-end (left, L) consisted of a *HindIII* fragment of approximately 0.6 kb, while the downstream 3'-end probe (right, R) was a 450 bp PCR-generated fragment (using the primers 5'-GGTCTGCATCAAGCCTGCC-3' and 5'-CTGAGCATAGCACAGAGAAAG-3'). In addition, a 1.8 kb *BglII* fragment of the PGK-hygromycin gene was used as hybridization probe (Hooper et al., 1987; Umans et al., 1994, 1995). One positive clone was identified from a screen of 241 clones, expanded and subsequently electroporated with 50 μ g of circular PGK-Cre plasmid (cre recombinase under the control of the PGK promoter). The cells were trypsinized after 2 days and plated in a dilution of 100 to 900 cells/25 cm² flask. 504 colonies were picked, expanded and plated in triplicate: 1 set of cells was subjected to hygromycin B selection (dying cells indicate correctly recombined clones), 1 set of cells was used for DNA preparation and the final set of cells was kept in culture. For screening purposes, a PCR reaction was performed on 422 clones using the primers indicated in Fig. 1A: construct-F (5'-ATATACTAGGTTAAGCGTGCTG-3') and construct-R (5'-GGATCAGGACAAACAGCTGC-3'). Eighteen clones were chosen for further analysis using Southern blotting with the three probes described above. Eleven correctly recombined clones were reconfirmed by Southern blotting, after which 4 ES cell lines were injected into C57Bl/6J blastocysts and transferred into pseudopregnant foster mothers. Three chimeric mice were born and mated to C57Bl/6J partners. Germ-line transmission was

achieved with a single chimera, which was subsequently mated to CBA/Ca in addition to the C57Bl/6J mating.

Genotyping mice

Tail-biopsy DNA was extracted using standard procedures. Founder mice and their offspring were genotyped by Southern

blotting as described above. Routine genotyping was performed by PCR using the construct-F and -R primers, amplifying a PCR product of 953 bp for wild-type and of 254 bp for mutant alleles. In addition, a second PCR reaction was performed routinely using an internal exon 8 PCR primer (exon8-F) together with construct-R primer, resulting in a PCR product of 476 bp if at least 1 wild-type allele was present.



RT-PCR and real-time RT-PCR

Total RNA was isolated from brain derived from wild-type, heterozygous and homozygous *Dfna5* mice using a Mini-Beadbeater (Biospec Products, Bartlesville, OK) in combination with Trizol (Invitrogen Life Technologies, Carlsbad, CA). Total RNA from inner ears from newborn *Dfna5*^{-/-} and *Dfna5*^{+/+} mice was prepared with the Rneasy minikit (Qiagen, Hilden, Germany). cDNA was prepared using random hexamers of the Superscript Preamplification System (Invitrogen Life Technologies, Carlsbad, CA). The presence of aberrant cDNA in mutant mice was investigated with a forward primer from exon 7 (5'-GCACCTA-GAGAGGAGTTTC-3') and a reverse primer from exon 10 (5'-GCAAGAGTCCTCAGGATGG-3'). To confirm the deletion of exon 8 in mutant cDNA, PCR products were purified using the QIAquick Gel Extraction Kit (Qiagen, Hilden, Germany) and subsequently sequenced.

To detect relative *Ugdh* levels, quantitative real-time RT-PCR was performed using TaqMan Assays-on-Demand (Applied Biosystems, Foster City, CA) for *Ugdh*, *Hprt* and *Hmbs* on an ABI PRISM 7900HT sequence detection system (Applied Biosystems, Foster City, CA). *Hprt* and *Hmbs* were chosen as household genes according to Vandesompele et al. (2002). Two separate biological samples were available per mouse genotype. For each biological sample, two different dilutions were pipetted in triplicate. The complete experiment was repeated once.

Dfna5 antiserum

Mouse *Dfna5h* cDNA was PCR cloned into the *Bam*HI restriction site of the pET15b vector (Novagen Inc., Madison, WI) to create an N-terminal fusion protein with a cleavable His-tag using the following primer pair 5'-ATGCTCGAGGATCC-GATGTTTGCCAAAGCAACTCG-3' and 5'-AGCAGCCGGATC-CTCCTAGTCTTGACCTGTAGCATG-3' and the previously cloned *Dfna5h* as template (Van Laer et al., 1998). The complete insert was bidirectionally sequenced to exclude the introduction of cloning errors. Expression was induced in the BL21(DE3)pLysS *E. coli* host strain according to the pET System Manual (Novagen Inc., Madison, WI). Cells were fractionated using Bugbuster Protein Extraction Reagent (Novagen Inc., Madison, WI) according to the manufacturer's instructions (pET System Manual), and protein fractions were subjected to Western blotting with Anti-His-tag Monoclonal Antibody (Novagen Inc., Madison, WI) as primary antibody. *Dfna5* recombinant protein was detected in the inclusion

body-containing fraction. Subsequently, large-scale induction of expression and isolation of inclusion bodies followed by His-Bind metal chelation chromatography under denaturing conditions using a His-Bind purification Pack (Novagen Inc., Madison, WI) was performed. Renaturation of the purified recombinant *Dfna5* was attempted by dialyzing with 6.5 mM CHAPS (Roche, Basel, Switzerland). Polyclonal antiserum against purified renatured recombinant *Dfna5* was generated using standard procedures at Eurogentec (Seraing, Belgium).

Western blot analysis

Brains derived from wild-type, heterozygous and homozygous *Dfna5* mice were homogenized in ST buffer (0.3 M sucrose, 1 mM EGTA, 10 mM Tris-HCl pH 7.4) in the presence of protease inhibitors (Complete Mini EDTA-free Protease Inhibitor Cocktail Tablets, Roche, Basel, Switzerland) using a Mini-Beadbeater (Biospec Products, Bartlesville, OK). Homogenates were centrifuged during 30 min at 30000 × *g* in a cooled Eppendorf centrifuge (Eppendorf, Hamburg, Germany). Pellets were resuspended in ST buffer containing protease inhibitors and protein concentrations were determined with the Coomassie Plus Protein Assay Reagent (Pierce, Rockford, IL). Protein concentrations were adjusted to 2 mg/ml and an equal volume of 2 × Laemmli loading buffer was added (Laemmli, 1970; except that 2-mercaptoethanol was replaced by dithiothreitol). The samples were subjected to SDS-PAGE and electrophoretically transferred to nitrocellulose membranes (Towbin et al., 1979) with a Multiphor II Novablot System (Amersham Pharmacia Biotech, Uppsala, Sweden). After blocking the membrane for 1 h with 5% non-fat milk powder (Nestlé, Vevey, Switzerland) in phosphate buffered saline containing 0.05% Tween-20 (PBST), the primary *Dfna5* antiserum was diluted 500 times in PBST containing 0.5% non-fat milk powder and incubated overnight. Immunodetection of *Dfna5* was performed with Blotting Grade Goat Anti-Rabbit IgG Horseradish Peroxidase Conjugate (Bio-Rad, Hercules, CA) diluted 10,000 times in PBST with 0.5% non-fat milk powder as secondary antibody, and the Western Lightning™ Chemiluminescence Reagent (Perkin-Elmer Life Sciences, Boston, MA) detection kit according to the manufacturer's instructions.

Auditory Brainstem Response (ABR)

Auditory brainstem responses (ABR) were recorded in anesthetized mice in a sound proof chamber (IAC). Anesthesia was

Fig. 1. Targeted mutagenesis of *Dfna5* and expression analysis. (A) Restriction map of the exon 8 region of wild-type *Dfna5*, the targeting construct and the targeted *Dfna5* locus after homologous recombination, before and after Cre recombinase treatment. The hygromycin resistance gene (HYG) was inserted in the reverse direction, as indicated by an arrow, replacing exon 8. After selection and analysis for correct targeting, the hygromycin resistance gene was deleted by Cre recombinase. The gray bars represent genomic DNA, the white boxes indicate exons. The thin line represents vector DNA. The black triangles represent *LoxP* sites. The left (L) and right (R) probes are indicated with double-sided arrows, while PCR primers are indicated with single sided partial arrows. H, *Hind*III; S, *Sst*I; M, *Mun*I; B, *Bsp*119I; Sa, *Sal*I. (B to E) Verification of correct targeting by Southern blotting of *Sst*I-digested genomic DNA from wild-type and targeted cell lines and hybridization with the L (C and E) and R (B and D) probes, before (B and C) and after (D and E) Cre recombinase treatment. Before Cre recombinase treatment, probe R generates a 6 kb and a 9.3 kb fragment for wild-type and mutant alleles respectively, while probe L hybridizes to fragments of 2.2 kb and 3.3 kb for the wild-type allele and to fragments of 9.3 kb and 3.3 kb for the mutant allele. After Cre recombinase treatment, probe R generates a 7.3 kb fragment, while probe L hybridizes to fragments of 7.3 kb and 3.3 kb for mutant alleles. (F) RT-PCR analysis of *Dfna5* mRNA. Primers were designed from exon 7 and exon 10. The expected PCR product of 565 bp is generated in *Dfna5*^{+/+} and *Dfna5*^{+/-} mice, while the mutant allele (in *Dfna5*^{+/-} and in *Dfna5*^{-/-} mice) produces a fragment of 363 bp lacking exon 8. M, 100 bp marker; B, blanc, i.e. PCR reaction without template. (G) Verification of *Dfna5* deficiency by Western blot analysis of brain protein from *Dfna5*^{+/+}, *Dfna5*^{+/-} and *Dfna5*^{-/-} mice stained with an anti-recombinant *Dfna5* antibody. *Dfna5* is indicated with an arrow. In addition, a non-specific band recognized by the antibody is indicated with NS. An immunoreactive band is seen in *Dfna5*^{+/+}, as well as in *Dfna5*^{+/-} at the expected molecular weight of approximately 57 kDa. No immunoreactivity is seen in *Dfna5*^{-/-} mice. R indicates a positive control lane containing recombinant *Dfna5*. Recombinant *Dfna5* shows a slightly higher molecular weight when compared to wild-type *Dfna5* due to the presence of the His-tag.

achieved by intraperitoneal injection of 50 mg/kg ketamin hydrochloride (Ketamin 50 Curamed, CuraMED Pharma, Germany), 8 mg/kg xylazin hydrochloride (Rompun 290, Bayer Leverkusen, Germany) and 0.25 mg/kg atropine sulfate (Atropinsulfat, Braun, Germany). Stimulus generation and response recordings were made using a National Instruments Multi IO Card (MIO 16 E1). Clicks with a duration of 100 μ s of alternating phase or tone pips of 3 ms duration (1 ms rise and fall time, cosine shaped) at a rate of 60/s with an alternating phase were presented in the free field with a Bayer DT 911 loudspeaker. Sound pressure was calibrated in situ at all recorded frequencies prior to each measurement (Bruel and Kjaer 4135, Nexus amplifier). To record the ABR potentials, subdermal silver wire electrodes were inserted at the vertex (reference), ventrolateral to the measured ear (active) and at the back (ground) of the mice. Electrical signals were averaged over 32 repetitions after amplification (100 dB) and bandpass filtering (0.3–5 kHz). Responses were recorded for frequencies between 2 and 45.2 kHz (2, 2.8, 4, 5.6, 8, 11.3, 16, 22.6, 32, 45.2), for each frequency from 20 to 100 dB SPL in 5dB steps. Only the right ear in each animal was tested. The software averager included an artifact rejection code (all waveforms with a peak-to-peak voltage exceeding a defined voltage were rejected) to eliminate the ECG and muscle activity. Thresholds were defined as the sound pressure level where a stimulus correlated response was clearly identified in the recorded signal. If no response was obtained, we used 110 dB SPL as threshold value for further calculations.

Vestibular tests

Air righting reflex

Mice were held on their back and subsequently dropped on a cushion from a height of 35 cm. If animals succeeded to turn during their fall and landed on their four paws, we concluded that the sacculus was functioning normal (Irwin, 1968; Steel and Hardisty, 1996).

Contact righting reflex

Mice were placed in a transparent plastic tube of 30 cm length and 3 cm diameter. Subsequently, the tube was rotated until the mice were lying on their back. Mice with normal vestibular reflexes turn inside the tube to get their bodies in an upward position again, while mice with vestibular dysfunction remain on their back (Steel and Hardisty, 1996).

Negative geotaxis

Mice were put with their head downward on a platform placed under an angle of 45°. Normal reacting mice turn and walk up the platform. Mice with vestibular problems walk down or fall off the platform (Steel and Hardisty, 1996).

Elevated platform

Mice were placed on a square platform (7 × 7 cm) at a height of 45 cm above a soft sub-soil. Mice showing vestibular dysfunction tend to fall sooner than normal mice. If the mice did not fall, they were removed from the platform after 2 min (Steel and Hardisty, 1996).

Reaching response

Mice were held by their tail above a flat surface and it was noted whether the forepaws were stretched out to make contact with the surface (normal response) or whether the mouse curled up

towards its tail (abnormal response) (Steel and Bock, 1983; Steel and Hardisty, 1996).

Swim test

Mice were placed in a plastic container filled with 30 cm of tepid water and observed during 2 min. Mice with vestibular dysfunction have problems swimming (Lyon et al., 1996; Steel and Hardisty, 1996).

Scanning electron microscopy

Adult mice were sedated with diethylether and killed by cervical dislocation. They were decapitated and inner ears were dissected and fixed immediately by immersion in ice-cold 2.5% glutaraldehyde in 0.1 M Na⁺-cacodylate. Under a stereomicroscope, both round and oval windows were opened in order to perfuse the perilymphatic compartment, followed by overnight immersion fixation in the same fixative at 4°C. Inner ears were rinsed in 0.1 M Na⁺-cacodylate containing 7.5% saccharose for at least 1 h, followed by perfusion with 1% OsO₄ in 0.033 M veronal-acetate containing 4% saccharose (pH 7.4) and postfixation by immersion in the same fixative for 1.5 h at room temperature (RT). Fixative was removed by rinsing the inner ears in 0.05 M veronal-acetate containing 6% saccharose (pH 7.4) three times for 15 min. Afterwards, cochleas were dissected under a stereomicroscope. Bone, stria vascularis and ligamentum spirale were removed, as well as Reissner's membrane and tectorial membrane. After dissection, cochleas were dehydrated by increasing concentrations of ethanol and critical-point dried. They were mounted with silverpaint and goldsputtered. Cochleas were studied with a SEM 515 scanning electron microscope (Philips, The Netherlands). Each cochlea was divided into two turns, the apical and the basal turn (Fig. 3A). Supernumerary hair cells and degenerations of hair cells (both OHCs and IHCs) were counted in each turn. To correct for damaged regions, an estimation of the portion with countable hair cells was made. To prevent the proliferation of large estimation errors, only those experiments were taken into account for statistical analysis for which the counted portion was at least 0.5. In the apical turn, a small portion near the helicotrema was not counted because of the normal irregularity of the hair cells in that area.

Explants of the organ of Corti

Newborn to 3-day-old mice were killed by decapitation and inner ears were dissected and immersed in sterile phosphate-buffered saline (PBS) containing 6 g/l glucose. The modiolus and the attached organ of Corti were dissected out and tissue surrounding the organ of Corti was removed. Organ of Corti explants was placed on the sterile membrane of a Millicell™ culture plate insert (0.4 μ m, 12 mm; Millipore, Bedford, MA) in minimal essential medium (MEM; Invitrogen Life Technologies, Carlsbad, CA) into a 24-well culture plate (Corning Inc., Corning, NY). Explants were kept in culture for 24 h at 37°C and 5% CO₂ and subsequently fixed during 7 min with 4% phosphate-buffered paraformaldehyde, permeabilized during 5 min by 1% Triton X-100 in PBS and blocked during 30 min by PBS containing 1.5% (w/v) non-fat milk powder (Nestlé, Vevey, Switzerland). All steps were carried out at room temperature (RT). Explants were stained with phalloidin-FITC (1 μ g/ml in PBS/milk powder; Sigma, St. Louis, MO) during 45 min at RT. After rinsing with PBS,

Millicell™ membranes supporting the organ of Corti explants were mounted using the SlowFade® Light Antifade kit (Molecular Probes Inc., Eugene, OR). Explants were studied using an epifluorescence microscope (Zeiss Axiophot; Zeiss, Germany) equipped with filters for visualization of FITC (Zeiss 17; BP 485–20/FT510/BP515–565). The total length of the explant was divided into three equal portions: apical, medial and basal (Fig. 4A). Supernumerary hair cells and degenerations of hair cells (both OHCs and IHCs) were counted in each portion. To correct for damaged regions, an estimation of the percentage of the portion with countable hair cells was made. Similar to the scanning electron microscopy counts described above, only those experiments with a countable portion of at least 0.5 were used for statistical analysis.

General histopathological analysis

Frimorfo (Fribourg, Switzerland), a specialized company, performed a general histopathological examination at the macroscopic and microscopical level of 46 organs (integument: skin and appendages; cardiovascular system: heart, aorta, vena cava; respiratory system: nose, larynx, trachea, lungs; immune/hemopoietic system: bone marrow, thymus, spleen, lymph nodes; digestive system: esophagus, stomach, small intestine, large intestine, salivary glands, liver and gallbladder, exocrine pancreas; male urogenital system: kidney, urinary bladder, testicles, epididymis and ductus deferens, male accessory sex glands, penis; musculoskeletal system: skeletal muscle (gastrocnemius muscle and soleus muscle), bone (tibia and vertebrae); endocrine system: pituitary gland, thyroid gland, adrenal gland, endocrine pancreas; central nervous system: cerebral cortex, hippocampus, basal ganglia, cerebellum, brainstem, spinal cord; peripheral nervous system: sciatic nerve, ganglia (trigeminal, dorsal root and autonomic ganglia); sensory organs: eye, eye accessory glands, ear, nose, tongue) in 1 *Dfna5*^{-/-} male and 1 *Dfna5*^{+/+} male littermate from the CBA/Ca genetic background. In addition, an external examination and an X-ray analysis were performed and a chemogram (7 metabolites, 5 enzymes and 1 electrolyte), hemogram (7 blood parameters, 6 blood cell counts and blood cell appearance) and urine profile were generated for 2 *Dfna5*^{-/-} and 2 wild-type littermates.

Histochemistry of hyaluronic acid

Hyaluronic acid was detected in 5 µm-thick paraffin sections of inner ears of both adult and young (postnatal day 1 or 2) wild-type and *Dfna5*^{-/-} mice. Sections were dewaxed, rehydrated and rinsed in PBS. To block endogenous peroxidase, slides were treated with 0.3% H₂O₂ in absolute methanol for 20 min. After rinsing in PBS, slides were incubated overnight at 4°C in biotinylated bovine nasal cartilage hyaluronic acid binding protein (B-HABP; Calbiochem/EMD Biosciences, La Jolla, CA, USA) diluted 1/100 in PBS containing 0.5 mg/ml bovine serum albumin (PBS/BSA). Sections were rinsed in PBS and incubated for 30 min in ExtrAvidin-horseradish peroxidase (Sigma, St. Louis, MO, USA) at a dilution of 1:1000 in PBS/BSA. Following rinsing in PBS, peroxidase activity was visualized by a 7 min incubation with diaminobenzidine (Pierce, Rockford, IL, USA). Finally, sections were counterstained with Carazzi hematoxylin, dehydrated and mounted in Entellan (Merck, Darmstadt, Germany).

To test the specificity of the B-HABP binding, sections were treated as described above without B-HABP or pretreated with hyaluronidase (Sames et al., 2001). Twenty-two units hyaluronidase (Hase) from bovine testes (type I-S; Sigma, St. Louis, MO) were dissolved in 0.02 M NaH₂PO₄ with 0.077 M NaCl and 0.01% BSA, pH 5.35. Parallel to the sections pretreated with Hase, sections were incubated with the same buffer lacking enzyme. After 3 h at 37°C, solutions were refreshed and slides were incubated for another 21 h at 37°C, followed by washing in PBS. To prevent background staining based on charge determined interactions, sections were treated with PBS containing 0.5% Aurion BSA-c (Aurion, Wageningen, The Netherlands) before B-HABP incubation.

Statistical analysis

To compare differences in hair cell counts in *Dfna5*^{+/+} and *Dfna5*^{-/-} mice, the Mann–Whitney rank sum test was calculated using SigmaStat 2.0 software (Jandel Corporation). To compare differences between threshold values of the ABR tests, a *t* test was performed using Excel (Microsoft). The results of the quantitative RT-PCR to detect relative *Ugdh* levels were statistically analyzed (*t* test) with SPSS 11.5 software. *P* values were taken significant at the 0.05 level.

Results

Generation of *Dfna5*^{-/+} and *Dfna5*^{-/-} mice

The gene-targeting strategy is illustrated in Fig. 1A. The first aim of this study was to mimic the human mutation in mouse. This was attempted through the deletion of exon 8 by targeted recombination in 129 ES cell lines. The second aim was to study the function of wild-type *Dfna5*. Therefore, an additional *LoxP* site was inserted before exon 7 to ensure the generation of a complete knockout mouse in case the deletion of exon 8 was insufficient. Correct targeting and Cre recombinase actions were verified by Southern blotting (Figs. 1B–E), after which blastocyst injections were initiated. One chimera showed germ-line transmission and was used for further breeding. As the 129 strain exhibits hearing loss itself, the genetic background was changed by crossing for 10 generations with C57Bl/6J, a strain with age-related hearing loss, and with CBA/Ca, a good-hearing reference strain. After 10 generations of breeding, 99.9% of the genome was derived from either C57Bl/6J or CBA/Ca. Homozygous mice were generated by mating heterozygotes from the 6th generation (98.4% of the genome derived from either C57Bl/6J or CBA/Ca) or from the 10th generation. Unless indicated otherwise, the experiments described in this paper were performed on animals of the 6th generation.

RT-PCR on mRNA from *Dfna5*^{+/+}, *Dfna5*^{+/-} and *Dfna5*^{-/-} (Fig. 1F) mice demonstrated the presence of aberrant mRNA in *Dfna5*^{+/-} and *Dfna5*^{-/-} mice. Direct sequencing of the 363 bp PCR fragment from *Dfna5*^{-/-} mice confirmed the absence of exon 8. Using Western blotting, the *Dfna5* immunoreactive band detected in *Dfna5*^{+/+} mice was approximately twice as intense as in *Dfna5*^{+/-} mice (Fig. 1G). No immunoreactivity was seen at the position of the predicted aberrant protein (approximately 49 kDa) in *Dfna5*^{+/-} or *Dfna5*^{-/-} mice (Fig. 1G), demonstrating that the *Dfna5* gene was effectively silenced. These data indicate that the aberrant mRNA found in *Dfna5*^{+/-} and *Dfna5*^{-/-} mice probably was destroyed through nonsense-mediated decay.

Auditory Brainstem Response (ABR)

To test the hearing impairment of *Dfna5* mice, click and frequency-specific ABR tests were performed on mice from the 2 different genetic backgrounds at different ages. It soon became clear that *Dfna5*^{+/-} mice did not show any significant hearing impairment (results not shown), and subsequent tests all concentrated on *Dfna5*^{-/-} mice in comparison to their wild-type littermates (Fig. 2). Because of the well-documented late-onset hearing loss of the

C57Bl/6J strain, *Dfna5* mice from the *C57Bl/6J* genetic background were only tested at 2 different ages: 4 to 5 months and 6 to 8 months. When compared to results derived from mice from the *CBA/Ca* genetic background, it is clear that *C57Bl/6J* mice hear significantly less than the good-hearing reference strain. For the higher frequencies (16 to 45.2 kHz), this was even clear at relatively young ages (4 to 5 months). In addition, the variation among animals from the *C57Bl/6J* strain is significantly larger than that from the *CBA/Ca* strain. *CBA/Ca* mice have excellent hearing abilities, even up to an

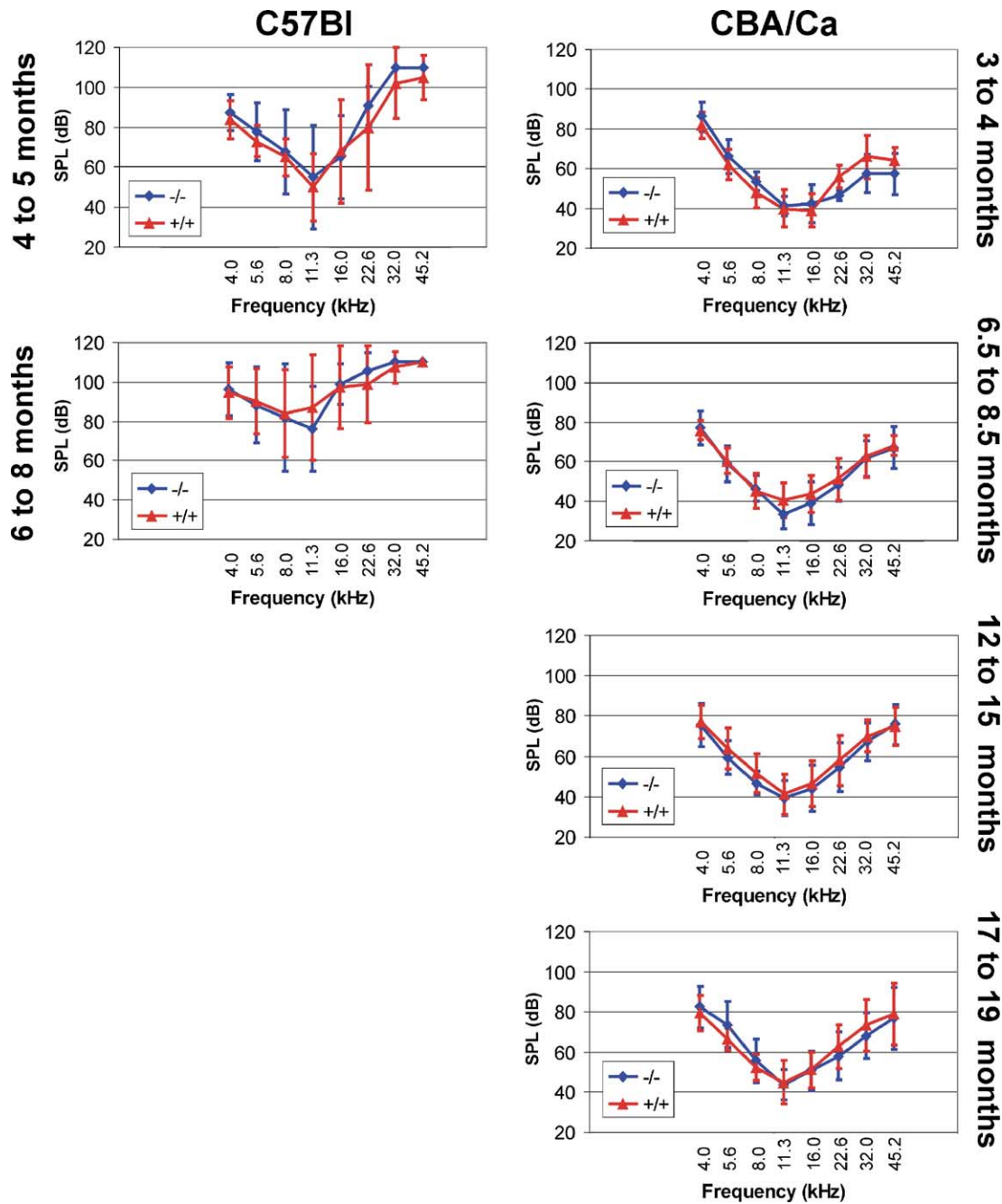


Fig. 2. Frequency-specific auditory brainstem response (ABR) of *Dfna5* knockout ($-/-$) mice and their wild-type littermates ($+/+$) in two genetic backgrounds. Mice of the *C57Bl/6J* genetic background were tested at an age of 4 to 5 months (143 ± 16 days) and 6 to 8 months (210 ± 22 days). Mice of the *CBA/Ca* genetic background were tested at an age of 3 to 4 months (101 ± 12 days), 6.5 to 8.5 months (221 ± 26 days), 12 to 15 months (399 ± 31 days) and 17 to 19 months (541 ± 23 days). The x axis indicates the different test frequencies, while the y axis indicates the sound pressure level (SPL). The results from 2 and 2.8 kHz were omitted from the figure.

age of approximately 1.5 years (Fig. 2). Even at this age, no significant differences could be detected between *Dfna5*^{+/+} and *Dfna5*^{-/-} mice.

Vestibular tests

A battery of simple vestibular tests (air righting reflex, contact righting reflex, elevated platform test, negative geotaxis test and swimming test) was performed on 21 *Dfna5*^{+/+}, 33 *Dfna5*^{+/-} and 15 *Dfna5*^{-/-} mice from the C57Bl/6J genetic background aged between 2 and 5 months (100 ± 22 days). Except for the air righting reflex and the swimming test, the tests were performed in duplicate. There were no differences between the performance of *Dfna5*^{+/+}, *Dfna5*^{+/-} and *Dfna5*^{-/-} mice in the different tests indicating that no major vestibular problems had arisen due to *Dfna5* deficiency (results not shown).

Scanning electron microscopy

Scanning electron microscopy was performed on mice aged 3 to 5.5 months from both genetic backgrounds (C57Bl/6J and CBA/Ca) (Fig. 3A). The cochlea was divided into 2 parts: an apical and a basal turn (Fig. 3B). Extra outer and inner hair cells and degenerations of outer and inner hair cells were counted in both turns, and counts

were corrected for the presence of damaged regions. For the basal part of the cochlea, only 6 *Dfna5*^{-/-} and 3 *Dfna5*^{+/+} preparations from the CBA/Ca genetic background passed the quality criterion (at least 1/2 turn countable), which did not lead to significant results (not shown). In the apical turn, no significant differences were detected for the extra inner hair cell counts or for the counts of degenerated inner and outer hair cells in the C57Bl/6J or in the CBA/Ca genetic background (results not shown). However, for the counts of fourth row outer hair cells in the apical turn of the cochlea, significant differences were observed between *Dfna5*^{+/+} and *Dfna5*^{-/-} mice in both genetic backgrounds (Fig. 3C). It is striking that the effect is opposite in the two genetic backgrounds: in the C57Bl/6J genetic background, *Dfna5*^{-/-} mice showed an increased number of fourth row outer hair cells when compared to wild-type littermates, while in the CBA/Ca genetic background, the number of fourth row outer hair cells was decreased in *Dfna5*^{-/-} mice when compared to *Dfna5*^{+/+} mice.

Explants of the organ of Corti

Explants of the organ of Corti of newborn mice were prepared from both genetic backgrounds (C57Bl/6J and CBA/Ca) (Fig. 4A). The explants were divided into three parts: an apical, a middle and

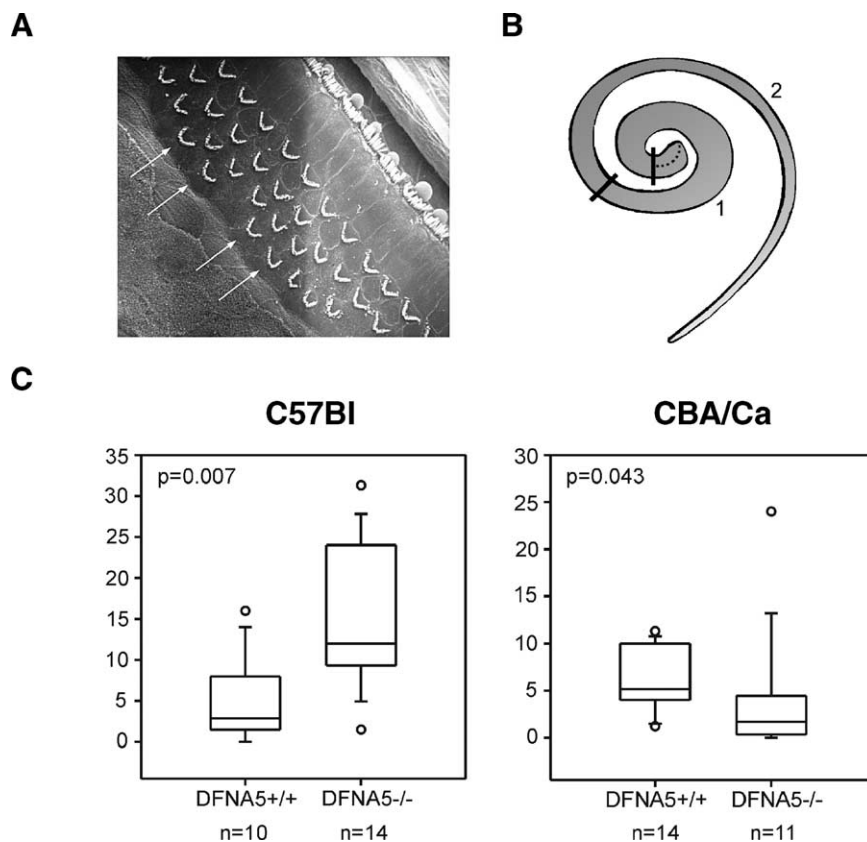


Fig. 3. Scanning electron microscopy of cochlear hair cells in the organ of Corti. A typical result is presented in panel A. The arrows indicate supernumerary (fourth row) outer hair cells, which were counted along the cochlear turns. (B) A diagram representing the division of the cochlea, for counting purposes, in an apical turn (turn number 1) and a basal turn (turn number 2). The portion near the helicotrema is indicated with a dotted line and was omitted from counting as the hair cell pattern is very irregular in this cochlear part. (C) Counts of fourth row outer hair cells in the apical turn of the cochlea in *Dfna5*^{-/-} mice and their wild-type littermates. For the C57Bl/6J experiments, mice were 3 to 5.5 months of age (116 ± 27 days), while the mice in the CBA/Ca genetic background were 3 to 5 months of age (119 ± 24 days). The rectangles of the box plots represent the 25 to 75 percentiles, the median is indicated as well. In addition, the 10 and 90 percentiles are given by the thin lines. All values outside the 10 to 90 percentiles are represented by small circles.

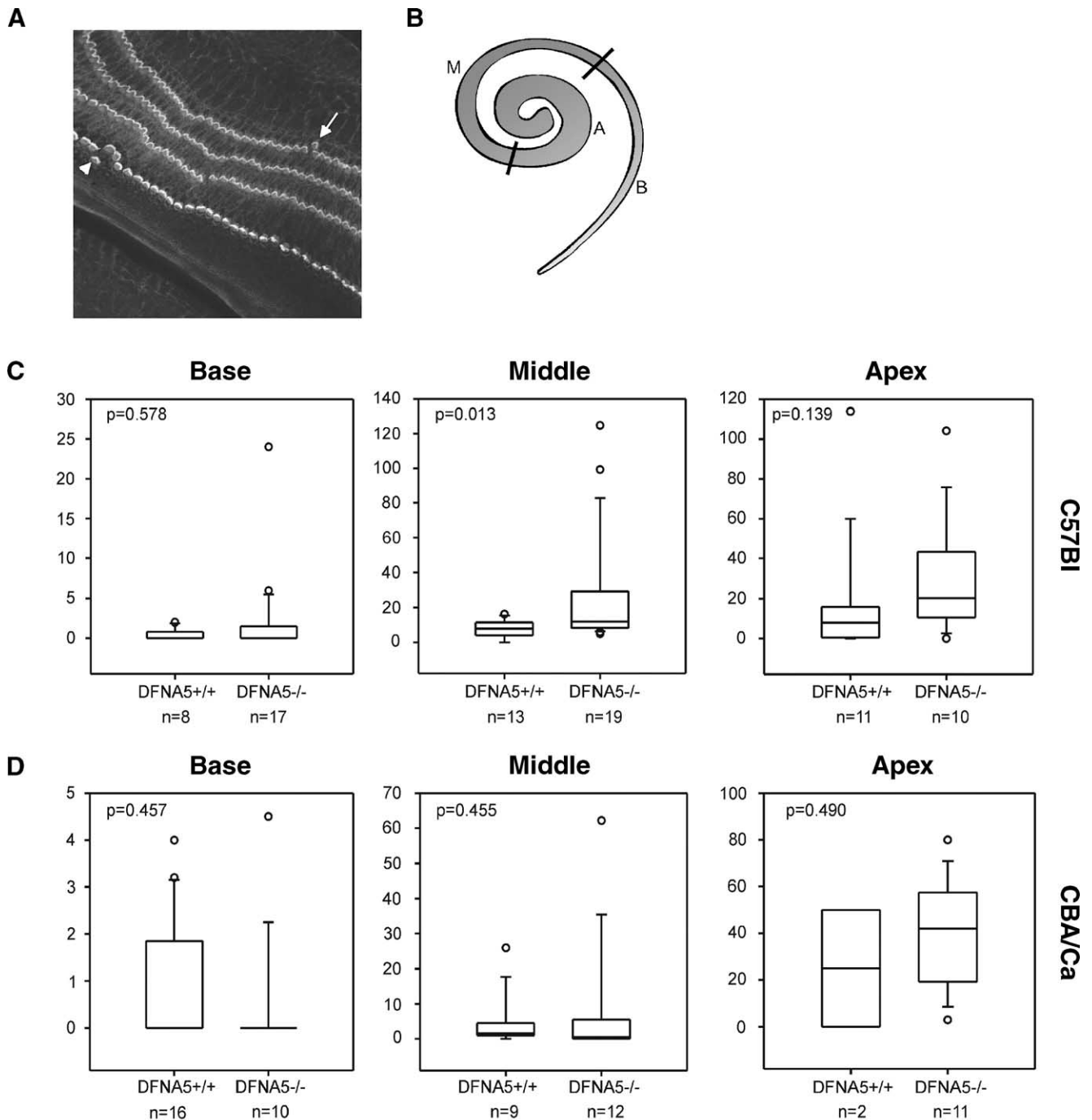


Fig. 4. Organ of Corti explants. A typical result is shown in panel A. The arrow indicates a fourth row outer hair cell, while the arrowhead indicates a supernumerary inner hair cell. (B) A diagram representing the division of the cochlea, for counting purposes, in an apical (A), a middle (M) and a basal (B) portion. (C–D) Counts of fourth row outer hair cells in 3 cochlear portions for *Dfna5*^{-/-} mice and their wild-type littermates in C57Bl/6J (panel C) and CBA/Ca (panel D) genetic background. The animals with C57Bl/6J genetic background in this figure were 10th generation homozygotes (*Dfna5*^{-/-}). Box plots have a similar structure as described in the legend to Fig. 3.

a basal portion (Fig. 4B), and extra outer and inner hair cells as well as degenerations of outer and inner hair cells were counted. Counts were corrected for damaged regions. No significant differences were observed in the counts of extra inner hair cells or in the counts of degenerated inner and outer hair cells in any of the three cochlear portions from the two genetic backgrounds (C57Bl/6J and CBA/Ca). However, in the C57Bl/6J genetic

background (Fig. 4C), significant differences between *Dfna5*^{+/+} and *Dfna5*^{-/-} mice were detected for extra outer hair cell numbers in the middle part of the cochlea, confirming the scanning electron microscopical findings. In addition, this trend is clearly visible in the apical portion of the cochlea. On the contrary, in the CBA/Ca genetic background (Fig. 4D), the scanning electron microscopy results could not be confirmed.

General histopathological analysis

As *Dfna5* expression could be demonstrated in every tissue investigated so far, a general histopathological examination was performed at macroscopical and microscopical level of 46 organs, including the ear. In addition, an external examination and an X-ray analysis were performed and a chemogram, hemogram and urine profile were generated. This extensive examination confirmed that the middle and inner ear of the *Dfna5*^{-/-} mouse have a normal structure and that at the light microscopical level no differences can be observed between *Dfna5*^{-/-} and *Dfna5*^{+/+} mice in the organ of Corti and the cochlear ganglion cells. No additional abnormalities were seen in any of the other 44 organs examined in the *Dfna5*^{-/-} mouse. In addition, X-rays were considered normal, and blood and urine values were within normal range.

Ugdh quantitative real-time RT-PCR and hyaluronic acid histochemistry

In *Dfna5* knockout zebrafish, a complete absence of UDP-glucose dehydrogenase (*Ugdh*) and a strong reduction in hyaluronic acid (HA) levels were demonstrated in the developing ear and pharyngeal arches. Therefore, we investigated the presence of *Ugdh* mRNA and HA in *Dfna5* knockout mice with quantitative real-time PCR and hyaluronic acid histochemistry, respectively. Relative *Ugdh* levels were measured in inner ear derived from newborn *Dfna5*^{-/-} and *Dfna5*^{+/+} mice, but no significant differences were obtained (Table 1).

HA expression was similar in adult and in newborn mouse inner ears and was concentrated in the extracellular matrix of the basilar membrane, in the limbus (mainly in the tympanic and vestibular lip) and the spiral ligament. Connective tissue surrounding the cochlea as well as the connective tissue core of the otolith organs and the cristae ampullaris were also positively stained (Fig. 5). HA staining was demonstrated in the cartilage of the bony cochlea of adult inner ears but was absent in the cartilage of young animals. In the control stainings without B-HABP or pretreated with HAse, no positive staining was observed. An identical expression pattern was observed in *Dfna5*^{+/+} and *Dfna5*^{-/-} mice, with no difference in staining intensity (Fig. 5).

Discussion

Dfna5 probably is an orphan gene and until recently nothing was known about its physiological function. Moreover, the pathophysiological mechanisms leading to hearing impairment were undeciphered. To shed light on both these matters, *Dfna5* mice that mimic the human mutation and lack *Dfna5* protein were generated. An additional *LoxP* site before exon 7 was included to generate a more upstream deletion if the deletion of exon 8 did not result in complete *Dfna5* deficiency. However, deletion of exon 8

gave no detectable protein and the more upstream deletion was not pursued. Based on our results, it is tempting to speculate that no aberrant protein is present in man in resemblance to the situation in mouse and that consequently hearing impairment in man is due to haplo-insufficiency. However, no experimental evidence to support this speculation could be gathered until now because of the scarcity of patient tissue material.

The *Dfna5* knockout mouse does not show hearing impairment and therefore does not mimic human hearing loss caused by mutations in *DFNA5*. Whether the *Dfna5*^{-/-} mouse mutant is more susceptible to noise-induced hearing loss or to hearing loss caused by other environmental factors remains unknown. The *Dfna5*^{-/-} mutant is not the first mouse with a targeted deletion of a gene known to cause human deafness that does not have a hearing loss phenotype. Mutations in Connexin31 (*GJB3*) cause autosomal dominant (*DFNA2*) or recessive non-syndromic hearing impairment (Liu et al., 2000; Xia et al., 1998), peripheral neuropathy in combination with hearing loss (Lopez-Bigas et al., 2001) or erythrokeratodermia variabilis (a skin disease; Richard et al., 1998). However, Connexin31 deficiency in mice does not lead to impaired hearing or skin abnormalities but causes transient placental dysmorphogenesis (Plum et al., 2001). A second example is the *Atp6b1*-null mouse. Mutations in human *ATP6B1* are responsible for distal renal tubular acidosis with sensorineural hearing loss (Karet et al., 1999). Although the *Atp6b1*^{-/-} mouse model does develop renal disease and resembles this aspect of the human disease, no hearing impairment was reported (Dou et al., 2003).

These types of phenotypic dissimilarity between a mouse model and the corresponding human disease may be due to (i) differences in physiology of the affected organs, (ii) different expression patterns of gene family members, if the gene in question belongs to a gene family, (iii) the genetic background, (iv) genetic redundancy or (v) differences in mutation type. For mutations affecting the cochlea, the first argument is not applicable. Only the inner ear is involved, and the physiological processes that occur in human and mouse inner ears are virtually identical. The second argument can also be rejected. *Dfna5* is believed to be an orphan gene and there are no data to suggest that a *Dfna5* family of genes exists. Obviously, the third argument (genetic background) cannot be ruled out. Although only little is known about the physiological pathways in which *Dfna5* functions, the possibility of genetic redundancy must also be considered. While genes acting in the same pathway may be able to complement the function of *Dfna5* in the *Dfna*^{-/-} mouse mutant and while the genetic background of mouse and man will surely be different, we believe that differences in the type of mutation best explain the lack of hearing impairment we have observed. We base this hypothesis on the identification of two additional mutations (Bischoff et al., 2004; Yu et al., 2003) in the *DFNA5* gene that cause hearing impairment. At the genomic DNA level, the three *DFNA5* mutations differ, however, at the mRNA level, all lead to exon 8 skipping indicating that only this specific event causes hearing impairment. This observation suggests that *DFNA5*-associated hearing loss is caused by a gain-of-function. Evidence supporting this hypothesis has been gained in yeast, where human mutant *DFNA5* has been shown to be toxic (Gregan et al., 2003). Consistent with this toxicity has been the finding of a detrimental function for human mutant *DFNA5* in mammalian cells (Van Laer et al., 2004).

The phenotypic differences between the two species may reflect the fact that, although the human mutation has been mimicked in the mouse, the human and mouse mutant proteins differ at their

Table 1
Average relative *Ugdh* mRNA levels in inner ear from newborn mice

Sample	<i>Ugdh</i> /Hprt ^a	<i>P</i> value	<i>Ugdh</i> /Hmbs ^a	<i>P</i> value
<i>Dfna5</i> ^{-/-} inner ear	3.92 ± 1.27	0.722	2.18 ± 0.82	0.128
<i>Dfna5</i> ^{+/+} inner ear	4.03 ± 0.67		1.87 ± 0.33	

^a *Ugdh*: UDP-glucose dehydrogenase; Hprt: hypoxanthine guanine phosphoribosyl transferase; Hmbs: hydroxymethylbilane synthase.

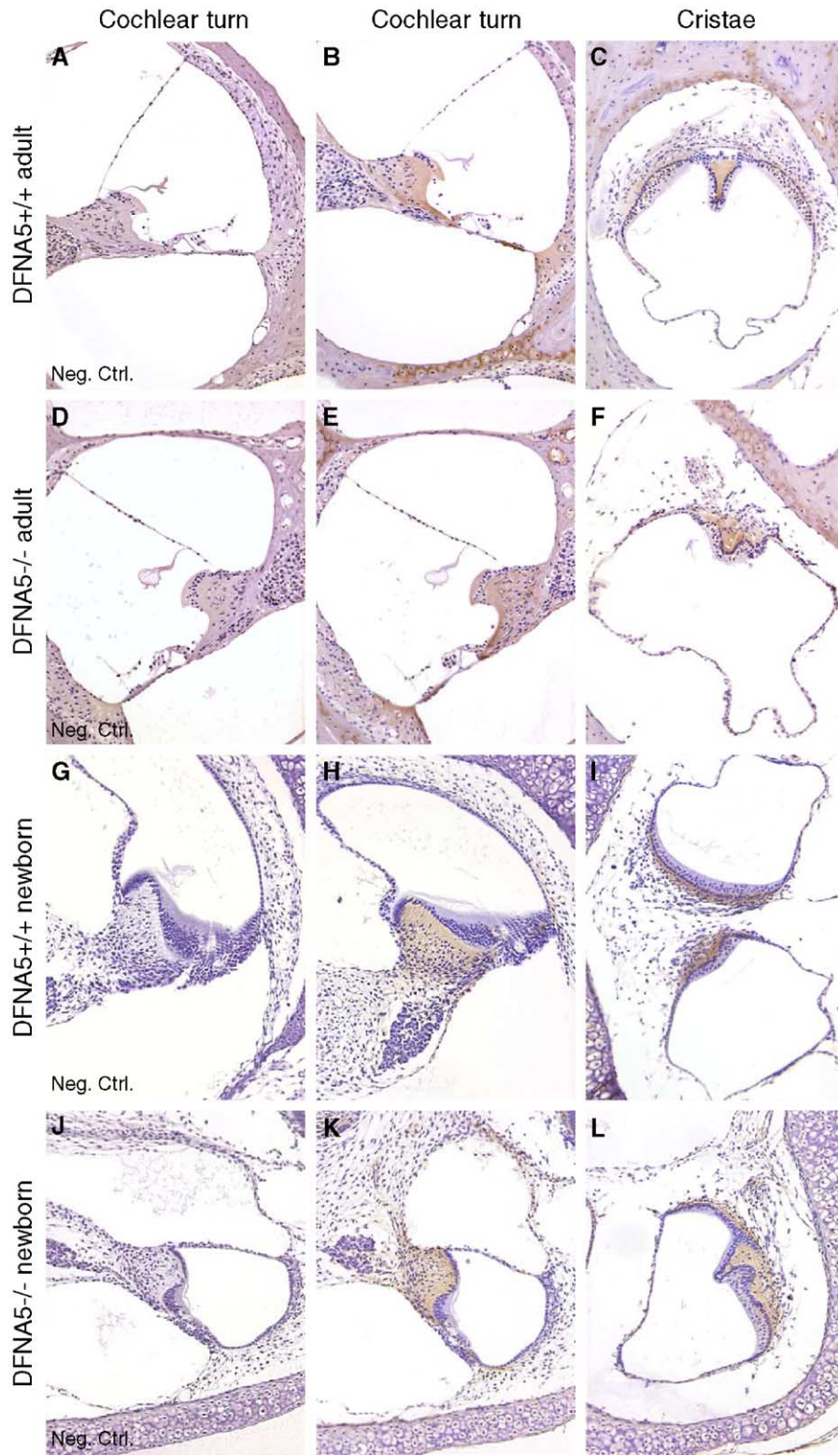


Fig. 5. Hyaluronic acid staining of *Dfna5* knockout ($-/-$) and wild-type ($+/+$) inner ears at two different ages (adult and newborn). For each stage, a cochlear turn (B and E for the adult stage, H and K for the newborn stage) and the cristae (C and F for the adult stage, I and L for the newborn stage) are shown for *Dfna5* $+/+$ (B, C, H and I) and *Dfna5* $-/-$ (E, F, K and L) mice. In addition, for each cochlear turn, a corresponding negative staining without B-HABP is given (A, D, G and J). The negative control for the cristae staining is not shown.

carboxy termini. Translation of mutant human and mouse mRNAs result in an aberrant stretch of 41 and 44 amino acids, respectively, that are significantly different. For this reason, human aberrant mRNA might escape detection by the nonsense-mediated decay machinery, while mouse aberrant mRNA does not. Alternatively, both mutant transcripts may be translated, followed by rapid degradation only of the murine protein. These possibilities mean that a transgenic mouse expressing human mutant *DFNA5* at physiological level would be a better model to study human hearing impairment than the knockout mouse described here.

Although the *Dfna5*^{-/-} mouse is not a suitable animal model for human hearing impairment, it may be a valuable tool to decipher the physiological function of *Dfna5*. The most striking finding we observed that suggests a putative function for wild-type *Dfna5* is the difference in numbers of extra outer hair cells between *Dfna5*^{+/+} and *Dfna5*^{-/-} mice. The organ of Corti is a highly organized mosaic of terminally differentiated sensory hair cells and non-sensory supporting cells, usually with a single row of inner hair cells and three rows of outer hair cells. However, irregularities in this highly ordered pattern exist. In primates, additional rows of outer hair cells are often observed, especially in the apical portion (Avan and Bonfils, 2003). In rodents, sporadic supernumerary inner and outer hair cells along the length of the cochlea are not uncommon. Four rows of outer hair cells occur at detectable and varying frequencies in different inbred mouse strains (Lim and Anniko, 1985), while the existence of extra inner hair cells has been systematically studied in rabbits (Borg and Viberg, 1995).

The differences in extra outer hair cell counts have been observed in adult mice and, at least in the C57Bl/6J genetic background, in newborn mice. The fact that the extra outer hair cells are present at birth may indicate that these cells develop together with the other inner and outer hair cells. The factors regulating the formation of the highly organized pattern of the organ of Corti are only partly known. Through the study of developmental defects resulting from targeted mutation, a number of genes have been implicated in inner ear morphogenesis and hair cell differentiation. A first set of genes regulating the differentiation of sensory hair cells in the vertebrate inner ear is a group of proteins operating in the Notch1 signaling pathway (Lanford et al., 1999; Zhang et al., 2000; Zine et al., 2000). *p27^{Kip1}*, an inhibitor of cell cycle progression, is another gene that is involved in organ of Corti development (Chen and Segil, 1999; Lowenheim et al., 1999). Finally, a series of regulator genes are essential for the formation of the strictly ordered cochlear mosaic. *Math1* is considered as a positive regulator of hair cell differentiation (Bermingham et al., 1999; Zheng and Gao, 2000), while *Hes1* and *Hes5* are believed to be downstream target genes of the Notch1 signaling pathway (Zheng et al., 2000; Zine et al., 2001). *Hes* genes can therefore influence cell fate by acting as negative regulators inhibiting the action of positive regulators (*Math1*). It is clear that the accurate control of both inner and outer hair cells is required for the generation of the regular mosaic pattern. A balance between positive and negative regulators is crucial for the production of an appropriate number of inner and outer hair cells. Whether *Dfna5* is another member of the Notch signaling pathway, involved in cell proliferation, or a regulator of hair cell differentiation remains to be elucidated. The generation of double knockout mice with *Dfna5* and members of the Notch signaling pathway or regulators of hair cell differentiation might give interesting clues.

Finally, it is possible that *Dfna5* might be involved in apoptosis as suggested before. In etoposide-resistant melanoma cell lines, it

was demonstrated that a reduction in *DFNA5* expression was associated with an increased etoposide resistance due to a decreased cellular susceptibility to trigger a caspase-3-dependent signaling pathway leading to programmed cell death (Lage et al., 2001). Kelley and others demonstrated that prosensory cells could be induced to become supernumerary hair cells during a limited period of time following terminal mitosis, which is accomplished without additional cell division. The latter would suggest that new cells are likely to have been derived either from cells that would otherwise have differentiated into supporting cells within the organ of Corti or from a population of cells that would normally have undergone apoptosis (Kelley et al., 1993; Lefebvre et al., 2000, 2001). If the latter suggestion holds, *Dfna5* might be involved in the process of programmed cell death during the formation of the mosaic structure of the organ of Corti. As a consequence, *Dfna5* deficiency might disturb normal patterning.

The differences in extra outer hair cell numbers between *Dfna5*^{-/-} and *Dfna5*^{+/+} mice are opposite in two genetic backgrounds: in the C57Bl/6J genetic background, *Dfna5*^{-/-} mice showed an increased number of fourth row outer hair cells when compared to wild-type littermates, while in the CBA/Ca genetic background, the number of fourth row outer hair cells was decreased in *Dfna5*^{-/-} mice when compared to *Dfna5*^{+/+} mice. This finding was unexpected but similar situations with knockout mice have been observed before. In fragile X (*Fmr1*) knockout mice bred in the C57Bl/6J genetic background, the size of the intra- and infra-pyramidal mossy fiber terminal fields (IIPMF) in the hippocampus was significantly reduced (Mineur et al., 2002), while the size of the IIPMF was significantly increased when the animals were bred in an FVB/N genetic background (Ivanco and Greenough, 2002). It is probable that for several developmental processes under multigenic control, the regulating balance might tip in one or the other direction depending on the genetic background against which a particular gene is acting.

A disorganization of the developing semicircular canals and a reduction of pharyngeal cartilage were observed in zebrafish *Dfna5* null mutants. These findings were correlated with a complete absence of UDP-glucose dehydrogenase (*Ugdh*) and a reduction in hyaluronic acid (HA) levels in the developing semicircular canals (Busch-Nentwich et al., 2004). In contrast, we did not detect any gross morphological abnormalities in the cochlea or vestibular system of *Dfna5*^{-/-} mice. In addition, *Ugdh* levels were not significantly different in newborn *Dfna5*^{-/-} mice when compared to *Dfna5*^{+/+} mice nor was the expression of HA reduced in *Dfna5*^{-/-} newborn or adult mice. This does not exclude a role for *Dfna5* in *Ugdh* regulation and HA biosynthesis. It could suggest, however, that *Ugdh* regulation and HA biosynthesis are more complex in mammals than in fish. *Ugdh* is a key enzyme in the biosynthesis of glycosaminoglycans, along which is HA. There is growing evidence that these glycosaminoglycans, besides being a major component of cartilage, also act in diverse aspects of cell behavior, such as signal transduction, cell proliferation, spreading, migration, tumor growth and metastasis (Iozzo and San Antonio, 2001; Toole et al., 2002). As such, glycosaminoglycans play a role in developmental, physiological and disease processes. Therefore, we cannot exclude that the differences we observed in supernumerary outer hair cells are correlated with slight differences in *Ugdh* regulation and consequently in glycosaminoglycan biosynthesis caused by the absence of *Dfna5*.

In conclusion, we have generated *Dfna5* knockout mice but could not detect significant hearing impairment or vestibular

dysfunction. Significant differences in the number of fourth row outer hair cells between *Dfna5*^{-/-} mice and their wild-type littermates were seen, albeit opposite in two genetic backgrounds. This finding may be indicative of a physiological function for *Dfna5*, which has to be further elucidated in future experiments.

Acknowledgments

We thank Dr. Brigitte Malgrange for helpful guidance into supernumerary hair cell matters and for teaching us how to prepare organ of Corti explants. LVL is a postdoctoral fellow of the Flemish Fonds voor Wetenschappelijk Onderzoek (FWO). This research was supported in part by a grant of the Geneeskundige Stichting Koningin Elisabeth (GSKE) to GVC and LVL, by an NOI-BOF grant of the University of Antwerp to LVL and by an FWO grant to GVC (G.0277.01N). This research was performed in the framework of the Interuniversity Attraction Poles programme P5/19 of the Belgian Federal Science Policy Office.

References

- Avan, P., Bonfils, P., 2003. Anatomy of peripheral auditory and vestibular systems. In: Luxon, L., Furman, J.M., Martini, A., Stephens, D. (Eds.), *Textbook of Audiological Medicine. Clinical Aspects of Hearing and Balance*. Taylor and Francis Group, London, pp. 3–11.
- Bermingham, N.A., Hassan, B.A., Price, S.D., Vollrath, M.A., Ben-Arie, N., Eatock, R.A., Bellen, H.J., Lysakowski, A., Zoghbi, H.Y., 1999. *Math1*: an essential gene for the generation of inner ear hair cells. *Science* 284, 1837–1841.
- Bischoff, A.M.L.C., Luijendijk, M.W.J., Huygen, P.L.M., van Duijnhoven, G., De Leenheer, E.M.R., Oudesluijs, G., Van Laer, L., Cremers, F.P.M., Cremers, C.W.R.J., Kremer, H., 2004. A second mutation identified in the *DFNA5* gene in a Dutch family. A clinical and genetic evaluation. *Audiol. Neuro-Otol.* 9, 34–36.
- Borg, E., Viberg, A., 1995. Extra inner hair cells: prevalence and noise susceptibility. *Hear. Res.* 83, 175–182.
- Busch-Nentwich, E., Sollner, C., Roehl, H., Nicolson, T., 2004. The deafness gene *dfna5* is crucial for *ugdh* expression and HA production in the developing ear in zebrafish. *Development* 131, 943–951.
- Chen, P., Segil, N., 1999. *p27Kip1* links cell proliferation to morphogenesis in the developing organ of Corti. *Development* 126, 1581–1590.
- Dou, H., Finberg, K., Cardell, E.L., Lifton, R., Choo, D., 2003. Mice lacking the B1 subunit of H⁺-ATPase have normal hearing. *Hear. Res.* 180, 76–84.
- Gregan, J., Van Laer, L., Lieto, L.D., Van Camp, G., Kearsy, S.E., 2003. A yeast model for the study of human *DFNA5*, a gene mutated in nonsyndromic hearing impairment. *Biochim. Biophys. Acta* 1638, 179–186.
- Hooper, M., Hardy, K., Handyside, A., Hunter, S., Monk, M., 1987. HPRT-deficient (Lesch-Nyhan) mouse embryos derived from germline colonization by cultured cells. *Nature* 326, 292–295.
- Iozzo, R.V., San Antonio, J.D., 2001. Heparan sulfate proteoglycans: heavy hitters in the angiogenesis arena. *J. Clin. Invest.* 108, 349–355.
- Irwin, S., 1968. Comprehensive observational assessment: Ia. A systematic quantitative procedure for assessing the behavioral and physiologic state of the mouse. *Psychopharmacology* 13, 222–257.
- Ivanco, T.L., Greenough, W.T., 2002. Altered mossy fiber distributions in adult *Fmr1* (FVB) knockout mice. *Hippocampus* 12, 47–54.
- Karet, F.E., Finberg, K.E., Nelson, R.D., Nayir, A., Mocan, H., Sanjad, S.A., Rodriguez-Soriano, J., Santos, F., Cremers, C.W.R.J., Di Pietro, A., Hoffbrand, B.I., Winiarski, J., Bakkaloglu, A., Ozen, S., Dusunsel, R., Goodyer, P., Hulton, S.A., Wu, D.K., Skvorak, A.B., Morton, C.C., Cunningham, M.J., Jha, V., Lifton, R.P., 1999. Mutations in the gene encoding B1 subunit of H⁺-ATPase cause renal tubular acidosis with sensorineural deafness. *Nat. Genet.* 21, 84–90.
- Kelley, M.W., Xu, X.M., Wagner, M.A., Warchol, M.E., Corwin, J.T., 1993. The developing organ of Corti contains retinoic acid and forms supernumerary hair cells in response to exogenous retinoic acid in culture. *Development* 119, 1041–1053.
- Laemmli, U.K., 1970. Cleavage of structural proteins during the assembly of the head of bacteriophage T4. *Nature* 227, 680–685.
- Lage, H., Helmbach, H., Grottko, C., Dietel, M., Schadendorf, D., 2001. *DFNA5* (ICERE-1) contributes to acquired etoposide resistance in melanoma cells. *FEBS Lett.* 494, 54–59.
- Lanford, P.J., Lan, Y., Jiang, R., Lindsell, C., Weinmaster, G., Gridley, T., Kelley, M.W., 1999. Notch signalling pathway mediates hair cell development in mammalian cochlea. *Nat. Genet.* 21, 289–292.
- Lefebvre, P.P., Malgrange, B., Thiry, M., Van De Water, T.R., Moonen, G., 2000. Epidermal growth factor upregulates production of supernumerary hair cells in neonatal rat organ of Corti explants. *Acta Oto-Laryngol.* 120, 142–145.
- Lefebvre, P.P., Malgrange, B., Thiry, M., Breuskin, I., Van De Water, T.R., Moonen, G., 2001. Supernumerary outer hair cells arise external to the last row of sensory cells in the organ of Corti. *Acta Oto-Laryngol.* 121, 164–168.
- Lim, D.J., Anniko, M., 1985. Developmental morphology of the mouse inner ear. A scanning electron microscopic observation. *Acta Oto-Laryngol.* 422, 1–69 (Suppl).
- Liu, X.Z., Xia, X.J., Xu, L.R., Pandya, A., Liang, C.Y., Blanton, S.H., Brown, S.D.M., Steel, K.P., Nance, W.E., 2000. Mutations in *connexin31* underlie recessive as well as dominant non-syndromic hearing loss. *Hum. Mol. Genet.* 9, 63–67.
- Lopez-Bigas, N., Olive, M., Rabionet, R., Ben-David, O., Martinez-Matos, J.A., Bravo, O., Banchs, I., Volpini, V., Gasparini, P., Avraham, K.B., Ferrer, I., Arbones, M.L., Estivill, X., 2001. *Connexin 31* (*GJB3*) is expressed in the peripheral and auditory nerves and causes neuropathy and hearing impairment. *Hum. Mol. Genet.* 10, 947–952.
- Lowenheim, H., Furness, D.N., Kil, J., Zinn, C., Gultig, K., Fero, M.L., Frost, D., Gummer, A.W., Roberts, J.M., Rubel, E.W., Hackney, C.M., Zenner, H.P., 1999. Gene disruption of *p27Kip1* allows cell proliferation in the postnatal and adult organ of Corti. *Proc. Natl. Acad. Sci. U. S. A.* 96, 4084–4088.
- Lyon, M.F., Rastan, S., Brown, S.D.M., 1996. *Genetic Variants and Strains of the Laboratory Mouse*. Oxford Univ. Press, Oxford.
- Marazita, M.L., Ploughman, L.M., Rawlings, B., Remington, E., Arnos, K.S., Nance, W.E., 1993. Genetic epidemiological studies of early-onset deafness in the U.S. school-age population. *Am. J. Med. Genet.* 46, 486–491.
- Mehl, A.L., Thomson, V., 1998. Newborn hearing screening: the great omission. *Pediatrics* 101, 1–6.
- Mehl, A.L., Thomson, V., 2002. The Colorado newborn hearing screening project, 1992–1999: on the threshold of effective population-based universal newborn hearing screening. *Pediatrics* 109, 1–8.
- Mineur, Y.S., Sluyter, F., de Wit, S., Oostra, B.A., Crusio, W.E., 2002. Behavioral and neuroanatomical characterization of the *Fmr1* knockout mouse. *Hippocampus* 12, 39–46.
- Morton, N.E., 1991. Genetic epidemiology of hearing impairment. *Ann. N.Y. Acad. Sci.* 630, 16–31.
- Plum, A., Winterhager, E., Pesch, J., Lautermann, J., Hallas, G., Rosentreter, B., Traub, O., Herberhold, C., Willecke, K., 2001. *Connexin31*-deficiency in mice causes transient placental dysmorphogenesis but does not impair hearing and skin differentiation. *Dev. Biol.* 231, 334–347.
- Rehm, H.L., 2003. Genetics and the genome project. *Ear Hear.* 24, 270–274.
- Richard, G., Smith, L.E., Bailey, R.A., Itin, P., Hohl, D., Epstein, E.H., DiGiovanna, J.J., Compton, J.G., Bale, S.J., 1998. Mutations in the human *connexin* gene *GJB3* cause erythrokeratoderma variabilis. *Nat. Genet.* 20, 366–369.
- Sames, K., Halata, Z., Jojovic, M., van Damme, E.J.M., Peumans, W.J., Delpech, B., Asmus, B., Schumacher, U., 2001. Lectin and proteogly-

- can histochemistry of feline pacinian corpuscles. *J. Histochem. Cytochem.* 49, 19–28.
- Steel, K.P., Bock, G.R., 1983. Cochlear dysfunction in the jerker mouse. *Behav. Neurosci.* 97, 381–391.
- Steel, K.P., Hardisty, R., 1996. Assessing hearing, vision and balance in mice. What's Wrong with My Mouse? *New Interplays Between Mouse Genes and Behavior. Soc. Neurosci. Short Course Syllabus*, Washington DC, pp. 26–38.
- te Riele, H., Robanus Maandag, E., Clarke, A., Hooper, M., Berns, A., 1990. Consecutive inactivation of both alleles of the *pim-1* proto-oncogene by homologous recombination in embryonic stem cells. *Nature* 348, 649–651.
- Toole, B.P., Wight, T.N., Tammi, M.I., 2002. Hyaluronan-cell interactions in cancer and vascular disease. *J. Biol. Chem.* 277, 4593–4596.
- Towbin, H., Staehelin, T., Gordon, J., 1979. Electrophoretic transfer of proteins from polyacrylamide gels to nitrocellulose sheets: procedure and some applications. *Proc. Natl. Acad. Sci. U. S. A.* 76, 4350–4354.
- Umans, L., Serneels, L., Hilliker, C., Stas, L., Overbergh, L., De Strooper, B., Van Leuven, F., Van den Berghe, H., 1994. Molecular cloning of the mouse gene coding for alpha 2-macroglobulin and targeting of the gene in embryonic stem cells. *Genomics* 22, 519–529.
- Umans, L., Serneels, L., Overbergh, L., Lorent, K., Van Leuven, F., Van den Berghe, H., 1995. Targeted inactivation of the mouse alpha 2-macroglobulin gene. *J. Biol. Chem.* 270, 19778–19785.
- Van Camp, G., Coucke, P., Balemans, W., van Velzen, D., van de Bilt, C., Van Laer, L., Smith, R.J.H., Fukushima, K., Padberg, G.W., Frants, R.R., Van de Heyning, P., Smith, S.D., Huizing, E.H., Willems, P.J., 1995. Localization of a gene for non-syndromic hearing loss (DFNA5) to chromosome 7p15. *Hum. Mol. Genet.* 4, 2159–2163.
- Van Laer, L., Huizing, E.H., Verstreken, M., van Zuijlen, D., Wauters, J.G., Bossuyt, P.J., Van de Heyning, P., McGuirt, W.T., Smith, R.J.H., Willems, P.J., Legan, P.K., Richardson, G.P., Van Camp, G., 1998. Nonsyndromic hearing impairment is associated with a mutation in DFNA5. *Nat. Genet.* 20, 194–197.
- Van Laer, L., Vrijens, K., Thys, S., Van Tendeloo, V.F.I., Smith, R.J.H., Van Bockstaele, D.R., Timmermans, J.P., Van Camp, G., 2004. DFNA5: hearing impairment exon instead of hearing impairment gene? *J. Med. Genet.* 41, 401–406.
- Vandesompele, J., De Preter, K., Pattyn, F., Poppe, B., Van Roy, N., de Paep, A., Speleman, F., 2002. Accurate normalization of real-time quantitative RT-PCR data by geometric averaging of multiple internal control genes. *Genome Biol.* 3, 1–12.
- Xia, J.H., Liu, C.Y., Tang, B.S., Pan, Q., Huang, L., Dai, H.P., Zhang, B.R., Xie, W., Hu, D.X., Zheng, D., Shi, X.L., Wang, D.A., Xia, K., Yu, K.P., Liao, X.D., Feng, Y., Yang, Y.F., Xiao, J.Y., Xie, D.H., Huang, J.Z., 1998. Mutations in the gene encoding gap junction protein beta-3 associated with autosomal dominant hearing impairment. *Nat. Genet.* 20, 370–373.
- Yu, C., Meng, X., Zhang, S., Zhao, G., Hu, L., Kong, X., 2003. A 3-nucleotide deletion in the polypyrimidine tract of intron 7 of the DFNA5 gene causes nonsyndromic hearing impairment in a Chinese family. *Genomics* 82, 575–579.
- Zhang, N., Martin, G.V., Kelley, M.W., Gridley, T., 2000. A mutation in the Lunatic fringe gene suppresses the effects of a Jagged2 mutation on inner hair cell development in the cochlea. *Curr. Biol.* 10, 659–662.
- Zheng, J.L., Gao, W.Q., 2000. Overexpression of *Math1* induces robust production of extra hair cells in postnatal rat inner ears. *Nat. Neurosci.* 3, 580–586.
- Zheng, J.L., Shou, J., Guillemot, F., Kageyama, R., Gao, W.Q., 2000. *Hes1* is a negative regulator of inner ear hair cell differentiation. *Development* 127, 4551–4560.
- Zine, A., Van De Water, T.R., de Ribaupierre, F., 2000. Notch signaling regulates the pattern of auditory hair cell differentiation in mammals. *Development* 127, 3373–3383.
- Zine, A., Aubert, A., Qiu, J., Therianos, S., Guillemot, F., Kageyama, R., de Ribaupierre, F., 2001. *Hes1* and *Hes5* activities are required for the normal development of the hair cells in the mammalian inner ear. *J. Neurosci.* 21, 4712–4720.